Available online at www.sciencedirect.com
ScienceDirect
Acta Materialia 56 (2008) 3414–3421
Acta MATERIALIA
www.elsevier.com/locate/actamat

Effect of nickel equivalent on hydrogen gas embrittlement of austenitic stainless steels based on type 316 at low temperatures

Lin Zhang [a], Mao Wen [a], Masaaki Imade [a], Seiji Fukuyama [a], Kiyoshi Yokogawa [b,*]

[a] Hydrogen Dynamics in Metals Research Team, Research Centre for Hydrogen Industrial Use and Storage, National Institute of Advanced Industrial Science and Technology (AIST), AIST Tsukuba Central 5-2, 1-1-1 East, Tsukuba 305-8565, Japan
[b] Research Institute of Instrumentation Frontier AIST, AIST Tsukuba Central 5-2, 1-1-1 East, Tsukuba 305-8565, Japan

Received 22 December 2007; received in revised form 11 March 2008; accepted 16 March 2008

Abstract

The effect of nickel equivalent on hydrogen gas embrittlement (HGE) of austenitic stainless steels of Fe–(10–20)Ni–17Cr–2Mo alloys vacuum-melted in a laboratory, based on type 316 stainless steel, was investigated. Tensile tests were conducted in hydrogen and helium at 1 MPa in the temperature range from 80 to 300 K. It was found that HGE of the alloys below a nickel equivalent of 27% increased with decreasing temperature, reached a maximum at 200 K, and then decreased with further decreasing temperature, whereas no HGE occurred above the nickel equivalent of 27%. It was observed that the content of strain-induced α' martensite increased with decreasing temperature and nickel equivalent, and hydrogen-induced fracture occurred mainly along α' martensite structure. Thus, the susceptibility to HGE depended on nickel equivalent. It was discussed that HGE was controlled by strain-induced α' martensite above 200 K, whereas it was controlled by hydrogen transport below 200 K.

Keywords: Stainless steel; Hydrogen embrittlement; Nickel; Low-temperature deformation; Tension test

1. Introduction

Hydrogen has recently been expected to be used as a source of clean energy, particularly as fuel for fuel cell vehicles (FCVs); thus hydrogen storage and transportation have become a key technology for FCVs. Hydrogen storage using liquid hydrogen is an important method of supplying hydrogen; thus the development of storage systems composed of storage tanks, containers and pipelines has been conducted throughout the world. Austenitic stainless steels are expected to be good candidates for the structural materials used in hydrogen storage systems based on liquid hydrogen. However, it is well known that austenitic stainless steels suffer from hydrogen embrittlement (HE). Stable austenitic stainless steels such as type 310 and 309 stainless steels were susceptible to HE when they were hydrogen-charged cathodically and thermally [1–10], but they showed no HE in hydrogen atmosphere, namely, hydrogen gas embrittlement (HGE) [4,7,11–15]. HE of hydrogen-charged stable austenitic stainless steels, in which no α' martensitic transformation occurred during deformation, can be attributed to the low stacking-fault energy of the steels, because the low stacking-fault energy inhibits cross slip and induces slip planarity [16,17]. Metastable austenitic stainless steels such as type 301, 304 and 316 stainless steels showed HE when they were hydrogen-charged [2–4,6–8,18–26] as well as HGE [4,5,7,11–15,27–32]; moreover, these materials suffered from HE due to strain-induced α' martensite [4,11,12,14,15,21,23,26,33,34]. The body-centered cubic (bcc) structure of α' martensite is inherently more susceptible to hydrogen-induced cracking than the face-centered cubic (fcc) structure in general, and it promotes hydrogen diffusion to accumulate in an embrittlement region at or near the crack tip; as Perng and Altstetter showed, α' martensite greatly enhanced the

* Corresponding author. Tel.: +81 29 861 4739; fax: +81 29 861 4845.
E-mail address: yokogawa.kiyoshi@aist.go.jp (K. Yokogawa).

1359-6454/$34.00 © 2008 Acta Materialia Inc. Published by Elsevier Ltd. All rights reserved.
doi:10.1016/j.actamat.2008.03.022

diffusivity of hydrogen in metastable austenitic stainless steels [34].

HE of austenitic stainless steels is temperature-dependent [1,6,7,9,10,15,18,20,26,31,32,35]. Wayman and Smith studied HE of thermally hydrogen-charged iron alloys containing 20% and 30% nickel [35]. HE was found to be severe at 293 K but was less remarkable at 77 K for the alloy containing 20% nickel; while for the alloy containing 30% nickel HE observed at 293 K did not occur at 77 K. Caskey studied the temperature dependence of HE of a wide variety of stainless steels including commercial and high-purity alloys [7]. It was found that HE of all hydrogen-charged alloys increased with decreasing temperature, reached a maximum between 200 and 300 K, and decreased with further decreasing temperature [7]. Buckley and Hardie [26] showed that the maximum HE of thermally hydrogen-charged 18Cr–11Ni stainless steel occurred at 215 K, and that no HE occurred below 160 K. Our recent studies [15,31,32] showed that HGE of commercially available austenitic stainless steels was also temperature-dependent and the maximum HGE of SUS 304 and 316 stainless steels [in the Japanese Industrial Standard (JIS)] in hydrogen at 1 MPa occurred at around 200 K, and that no HGE appeared below 120 K.

HE of austenitic stainless steels is also chemical-composition-dependent. Wayman and Smith demonstrated that HE of the iron–nickel alloy containing 20% nickel was severer than that of the alloy containing 30% nickel [35]. Caskey observed that nickel addition decreased the temperature of the strain-induced martensitic transformation in iron–chromium–nickel stainless steels and that HGE of the materials decreased markedly in the nickel composition range from 8% to 14% associated with an increase in austenite stability at room temperature [7]. The role of nickel is thus to improve both the stability of the austenitic phase and the resistance to HE; thus, the other alloy elements that promote the stability of the austenitic phase should improve the resistance to HE in general.

The degree of austenite phase stability against strain-induced α' martensitic transformation and the tendency of forming the austenite phase can be evaluated by nickel equivalent Ni_{eq}:

$$Ni_{eq} = Ni + 0.65Cr + 0.98Mo + 1.05Mn + 0.35Si + 12.6C \quad (1)$$

where all elements are in weight fractions [36]. It is evident that elements such as chromium, molybdenum, manganese, silicon and carbon promote the stability of the austenite phase. Thus, HE can be correlated with Ni_{eq}; however, the effect of Ni_{eq} on HE has not yet been clarified.

In this study, the effect of Ni_{eq} on HGE of Fe–(10–20)Ni–17Cr–2Mo alloys, based on type 316 stainless steel, was investigated in 1 MPa hydrogen and helium in the temperature range from 80 to 300 K. The relationship between HGE and α' martensite of the alloys was examined, and then the effect of Ni_{eq} on HGE of the alloys was discussed.

2. Experimental

The nickel content of the austenitic stainless steels of Fe–(10–20)Ni–17Cr–2Mo alloys, based on type 316 stainless steel, was changed from 10% to 20% to study the effect of Ni_{eq} on HGE. We name these alloys as melted type 316 stainless-steel alloys in this paper. The chemical compositions of the alloys, with Ni_{eq} from 24.20% to 34.33% according to Eq. (1), are listed in Table 1. The alloys were melted in a vacuum high-frequency induction furnace, and solution-annealed at 1373 K for 5 min after forging into round bars, and then machined into cylindrical tensile specimens with a gauge length of 20 mm and a diameter of 4 mm. The specimen surface was finally ground with sandpaper and polished with paste. Tensile tests were conducted in helium and hydrogen, the purities of which were 99.999% and 99.9999%, respectively, at 1 MPa in the temperature range from 80 to 300 K using our custom-developed equipment for studying HGE at low temperatures [37]. We investigated tensile behaviors of type 304 austenitic stainless steels in hydrogen and helium under a pressure of 1 MPa in the temperature range 80–300 K at strain rates ranging from 4.2×10^{-5} to 4.2×10^{-2} s^{-1} in our previous work [31]. It was shown that hydrogen played a marked role on HGE

Table 1
Chemical compositions of the melted type 316 stainless steels

Steel	Ni_{eq} (%)	Chemical composition (wt.%)								
		Ni	Cr	Mo	C	Si	Mn	P	S	Cu
316-1	24.20	9.88	17.00	2.07	0.010	0.50	0.90	0.025	0.001	0.25
316-2	25.24	10.97	16.90	2.08	0.010	0.50	0.90	0.027	0.001	0.25
316-3	26.45	12.11	17.00	2.08	0.010	0.48	0.91	0.025	0.001	0.26
316-4	27.17	12.90	16.96	2.05	0.010	0.50	0.89	0.025	0.001	0.26
316-5	28.29	13.90	17.11	2.03	0.013	0.47	0.91	0.025	0.001	0.26
316-6	29.18	14.88	16.98	2.07	0.009	0.49	0.90	0.026	0.001	0.25
316-7	30.27	15.90	17.07	2.06	0.010	0.51	0.90	0.026	0.001	0.27
316-8	31.31	16.96	17.05	2.06	0.010	0.52	0.90	0.027	0.001	0.27
316-9	32.42	18.07	16.96	2.12	0.010	0.52	0.90	0.026	0.001	0.27
316-10	33.41	18.98	17.08	2.10	0.011	0.52	0.91	0.026	0.001	0.27
316-11	34.33	19.93	17.08	2.08	0.009	0.52	0.92	0.026	0.001	0.27

at $4.2 \times 10^{-5}\ s^{-1}$, HGE decreased with increasing temperature and no HGE was observed at $4.2 \times 10^{-2}\ s^{-1}$. Thus, all tests were conducted with a strain rate of $4.2 \times 10^{-5}\ s^{-1}$ to ensure a reasonable effect of hydrogen on the mechanical properties of the materials in the present study. The fracture surface of the specimen after tensile tests was analyzed by scanning electron microscopy (SEM), and the content of strain-induced α' martensite in austenite, was measured by the magnetic method as ferrite equivalent. The foil for transmission electron microscopy (TEM) was prepared from the specimen deformed by a strain of 10%. The TEM foils were cut from the specimen, ground using sandpaper with water, perforated by final polishing and thinning using a twin-jet technique in an electrolyte consisting of an 8% solution of $HClO_4$ in ethanol, and then observed using by TEM (Hitachi H-9000).

3. Results

Typical stress–strain diagrams for the 316-1 (Ni_{eq} of 24.20%), 316-3 (Ni_{eq} of 26.45%) and 316-5 (Ni_{eq} of 28.29%) specimens tested in hydrogen and helium at 300, 200 and 80 K are shown in Fig. 1. It is evident that the yield stress of all specimens tested in helium increases whereas ultimate tensile stress (UTS) decreases with increasing nickel content. Hydrogen has a small effect on the 316-1 specimen at 300 K, as shown in Fig. 1a. Hydrogen induces the early fracture of the 316-1 and 316-3 specimens tested at 200 K, the elongations of which are rapidly reduced, and UTSs are reduced to almost the same level as that of the 316-5 specimen, as shown in Fig. 1b. Hydrogen exerts no effect on the stress–strain curves for the 316-3 and 316-5 specimens at 300 K shown in Fig. 1a, for the 316-5

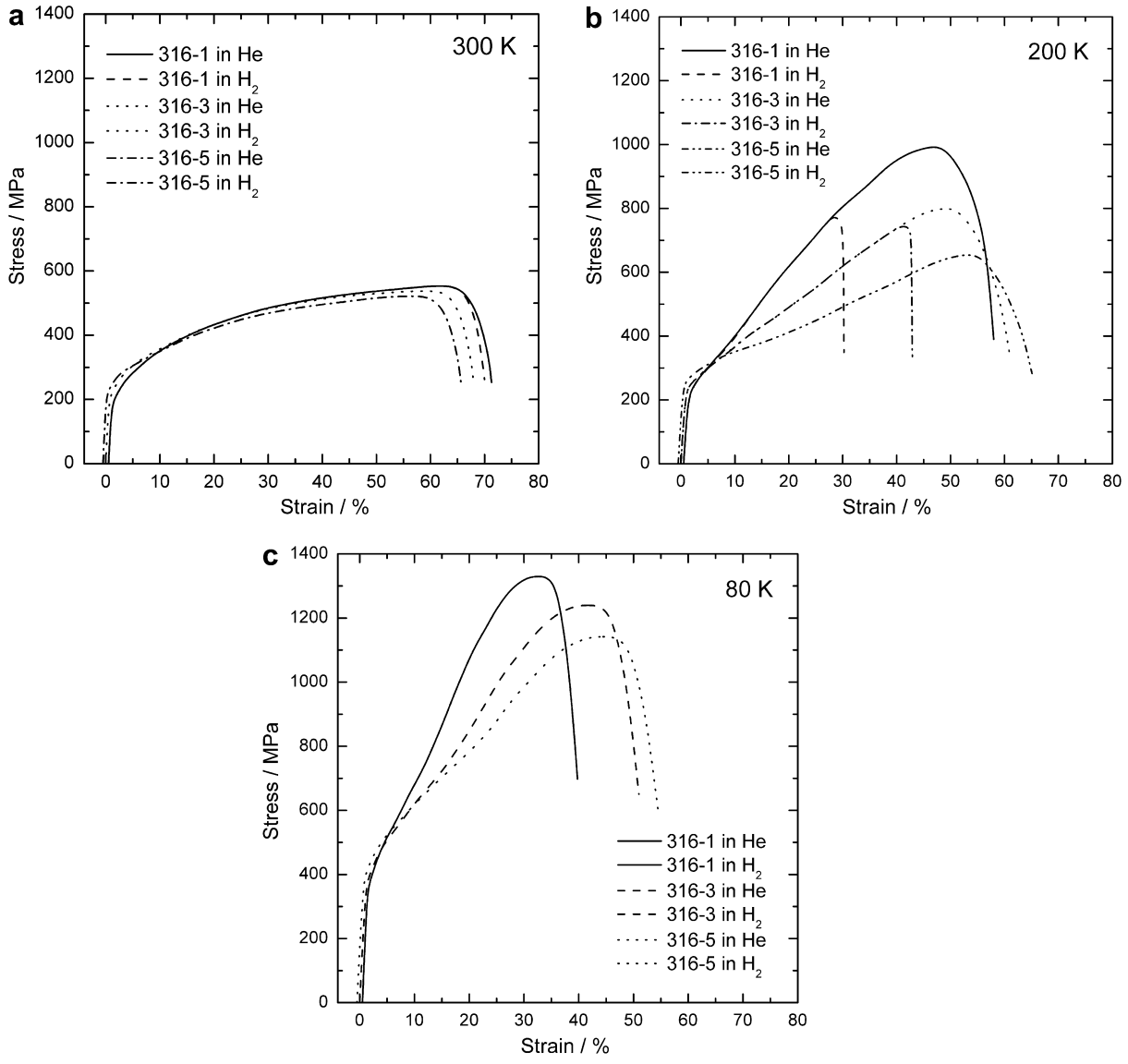

Fig. 1. Stress–strain curves of the 316-1, 316-3 and 316-5 specimens in 1 MPa hydrogen and helium at 300 K (a), 200 K (b) and 80 K (c).

specimen at 200 K shown in Fig. 1b and for all the specimens tested at 80 K shown in Fig. 1c.

HGE can be quantitatively described by the relative reduction of area (RRA), namely, the reduction of area measured in hydrogen at 1 MPa relative to that in helium at 1 MPa (reduction of area in H_2/reduction of area in He) [15], where no HGE is observed at an RRA of 1, and HGE increases with decreasing RRA. The dependence of RRA on testing temperature for the 316-1, 316-3 and 316-5 specimens is shown in Fig. 2. HGE is obviously dependent on alloy type and temperature, namely, the RRA of the 316-1 and 316-3 specimens decreases with decreasing temperature, reaches a minimum at 200 K and then increases with further decreasing temperature. This is in agreement with the result obtained by Caskey for thermally hydrogen-charged type 316 stainless steel [7] and our result for commercially available SUS316 stainless steel in a hydrogen environment at 1 MPa [15,31,32]. The error bar of the data of the specimens is shown at 200 K in particular, where minimum RRA is observed for the 316-1 and 316-3 specimens. No HGE is observed at the RRA of the 316-5 specimen.

The stability of austenitic stainless steels can be described by Ni_{eq}. The dependence of RRA on the temperature and Ni_{eq} of the alloys is shown in Fig. 3. The size of the symbols corresponds to that of the error bar shown in Fig. 2. The 316-1, -2 and -3 specimens only show HGE; namely, specimens below a Ni_{eq} of 27% show HGE, whereas those above the Ni_{eq} of 27% show no HGE at all temperatures tested.

The effect of temperature on the α' martensite content of all specimens is shown in Fig. 4. The ferrite equivalent near the fracture surfaces was measured by the magnetic method after the specimen fractured in helium and the maximum value of the measured values of the specimen is plotted in the figure. The ferrite equivalent measured in this way corresponds to the content of α' martensite in the fractured region. It is shown that the α' martensite content of the specimen with a Ni_{eq} of 24.20% increases with decreasing temperature until 200 K. The α' martensite content of the specimen with a Ni_{eq} of 28.29% is 0% above 250 K, and increases with decreasing temperature below 250 K, whereas no α' martensite exists in the specimen with a Ni_{eq} of 34.33% in the entire temperature range. The content of α' martensite decreases with increasing Ni_{eq} and temperature.

Since the most serious HGE occurs at 200 K, a sectional view of Fig. 3 at 200 K is shown together with the ferrite equivalent in Fig. 5. The size of the symbols corresponds to that of the error bar shown in Fig. 2. It is evident that RRA increases slowly with increasing Ni_{eq} from 24% to

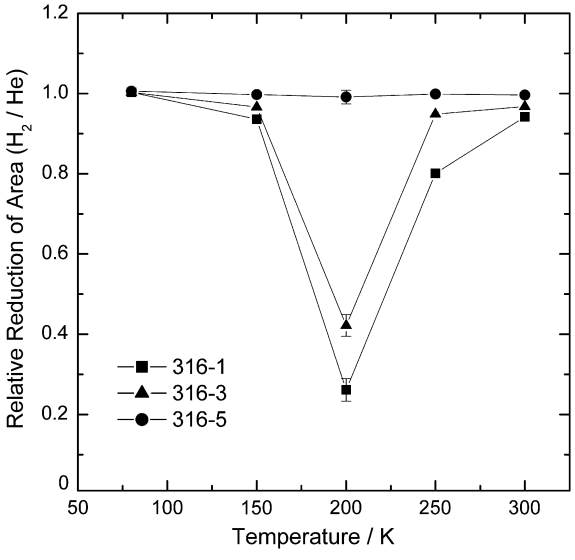

Fig. 2. Effect of temperature on relative reduction of area of the 316-1, 316-3 and 316-5 specimens in 1 MPa hydrogen and helium at low temperatures.

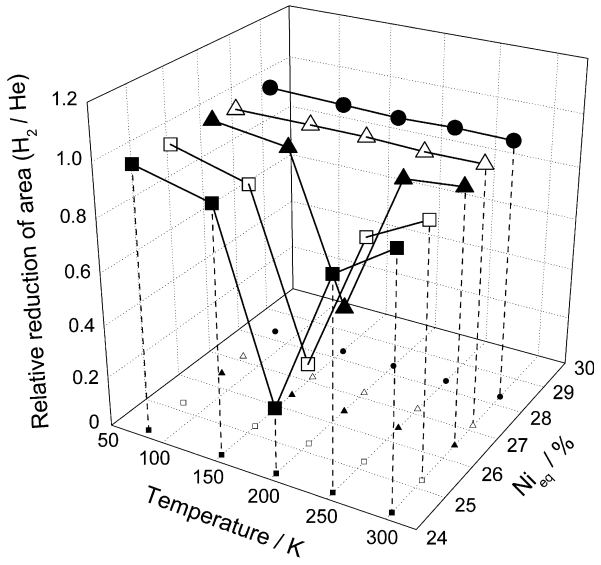

Fig. 3. Effect of temperature and nickel equivalent on relative reduction of area of melted type 316 stainless-steel alloys in 1 MPa hydrogen and helium at low temperatures.

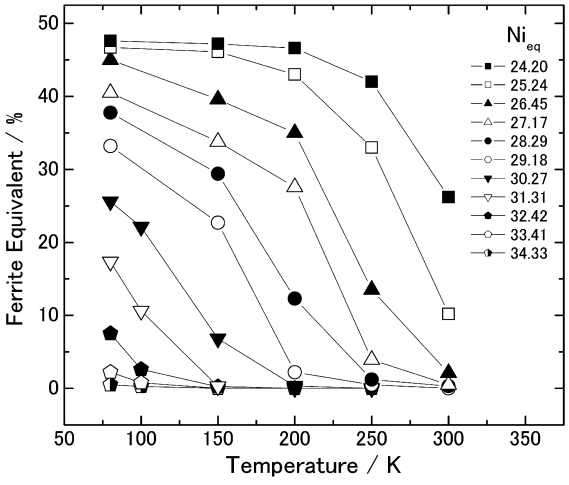

Fig. 4. Effect of temperature on ferrite equivalent of melted type 316 stainless-steel alloys at low temperatures.

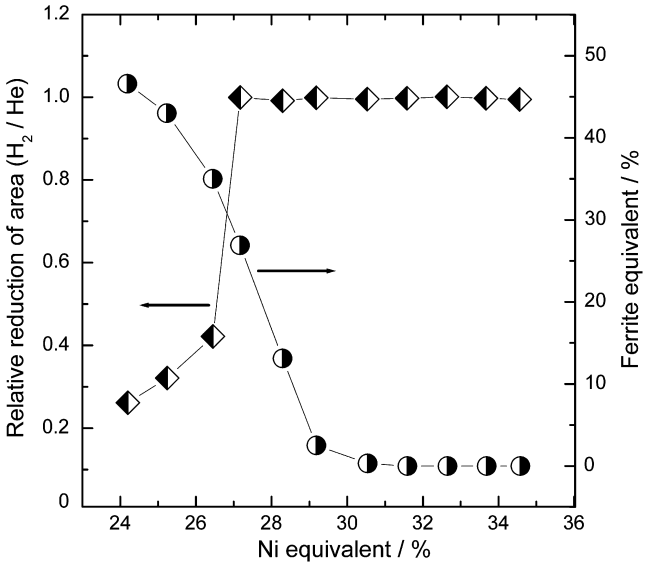

Fig. 5. Effect of nickel equivalent on relative reduction of area and ferrite equivalent of melted type 316 stainless-steel alloys in 1 MPa hydrogen and helium at 200 K.

26%, rapidly to 1 from 26% to 27%, and remains at 1 above 27%, where no HGE exists. Thus, HGE occurs below the Ni_{eq} of 27% and becomes more serious with decreasing Ni_{eq}. Whereas the ferrite equivalent of the alloy decreases from 47% to 0% in this Ni_{eq} range, the ferrite equivalent is still 28% and RRA is almost 1.0 at the Ni_{eq} of 27%. It is evident that an increase in Ni_{eq} decreases the susceptibility of the alloys to HGE.

Fracture surfaces, observed by SEM, of the 316-1, 316-3 and 316-5 specimens tested in hydrogen at 1 MPa at 200 K are shown in Fig. 6. The observations were focused on the sites near surfaces where cracks initiated. Transgranular fractures along strain-induced martensite structure were mainly observed and flat facets due to twin-boundary separation were also observed in the 316-1 specimen, which are typical hydrogen-induced fracture modes, as shown in Fig. 6a. Transgranular fractures along strain-induced martensite structure were only observed in the 316-3 specimen, as shown in Fig. 6b. Dimple rupture was observed in the 316-5 specimen, as shown in Fig. 6c. Dimple rupture was also observed in all specimens tested in helium and the specimens above the Ni_{eq} of 27% tested in hydrogen at all temperatures.

The microstructure of deformed specimens was observed by TEM. Bright-field TEM images and selected-area diffraction (SAD) patterns of the 316-3 specimen deformed by a strain of 10% in helium at various temperatures are shown in Fig. 7. The austenite phase, identified from the SAD pattern, was only observed at 300 K, as shown in Fig. 7a, indicating that α' martensitic transformation did not occur. Strain-induced α' martensite identified from the SAD pattern has a three-dimensional structure and appeared at intersections of the microscopic slip bands constituting of stacking faults and ε martensite at 200 and

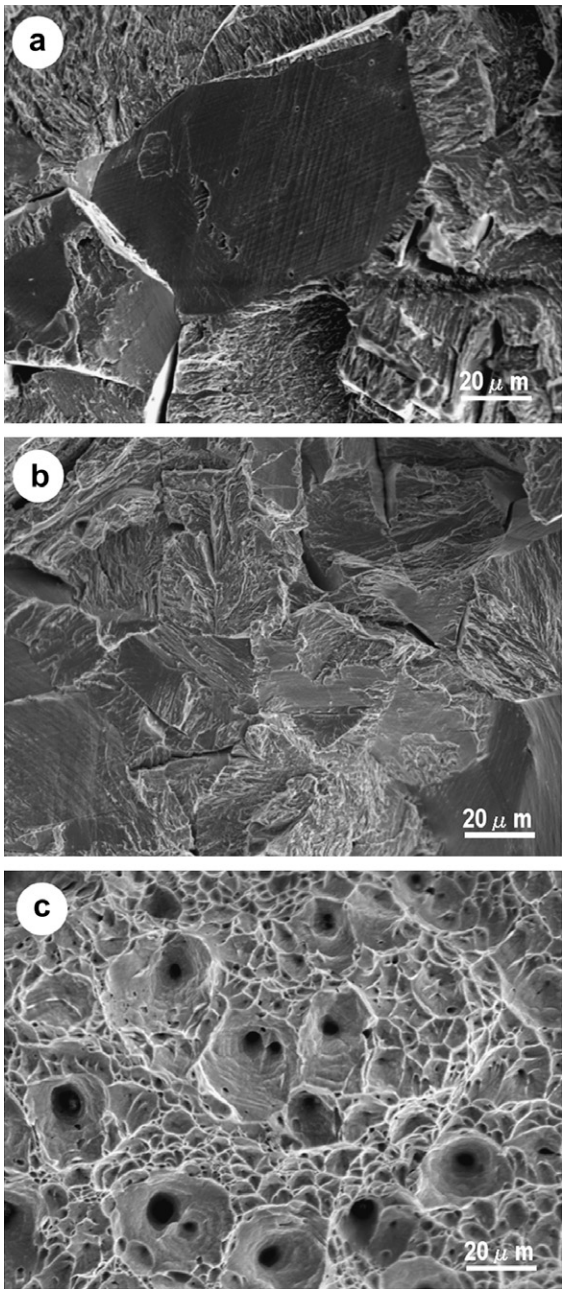

Fig. 6. Fracture surfaces of the 316-1 (a), 316-3 (b) and 316-5 (c) specimens fractured in 1 MPa hydrogen at 200 K.

80 K in accordance with our previous paper [15], as shown in Fig. 7b and c.

4. Discussion

HGE may occur when a hydrogen-free material is mechanically tested in gaseous hydrogen environment, where hydrogen molecules adsorb on the surface and decompose into atomic hydrogen, and the hydrogen atoms migrate across the surface, dissolve and diffuse into the material [38]. It was shown by Troiano [39] that HE of steels occurs by crack propagation in a discontinuous

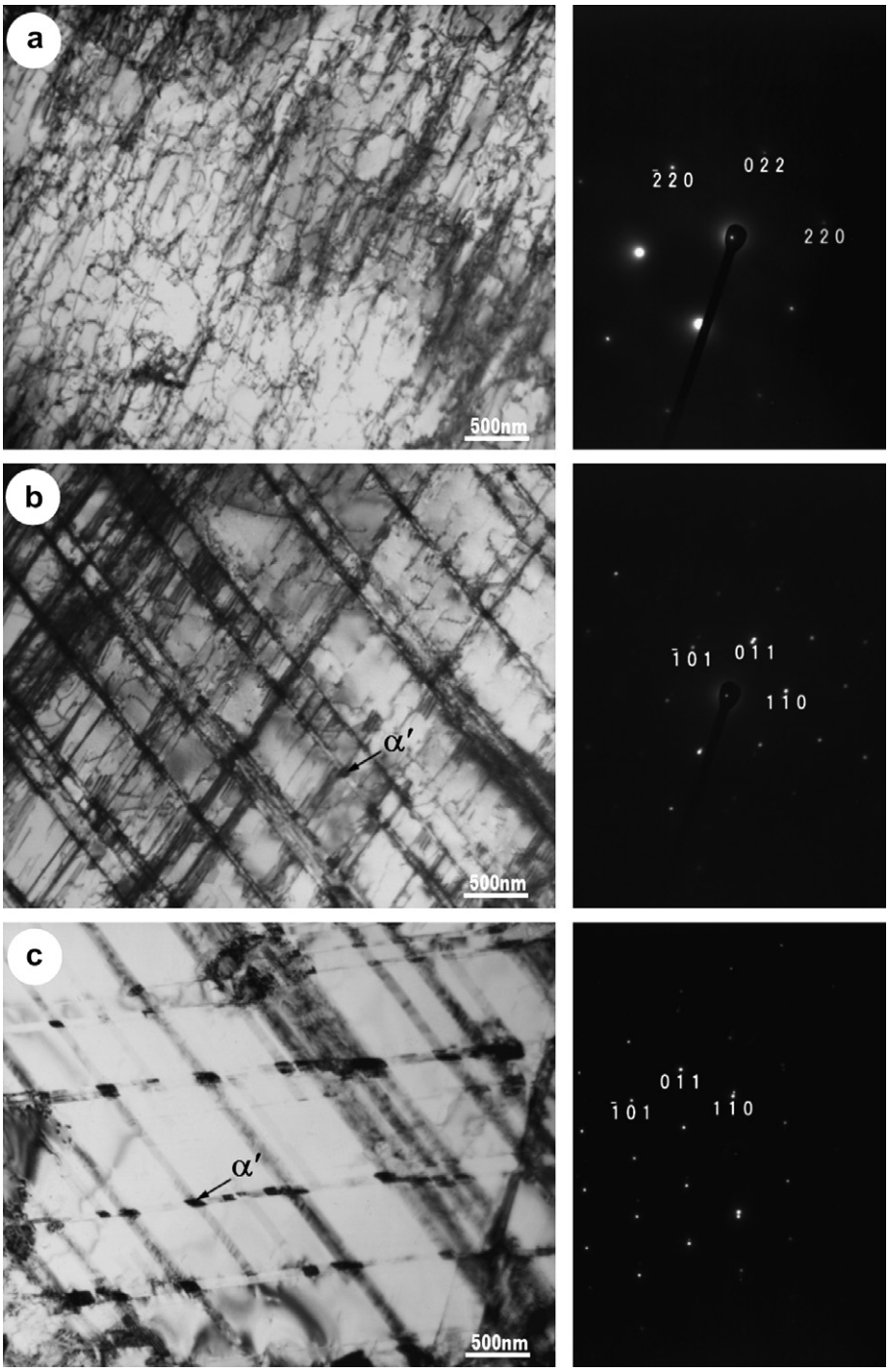

Fig. 7. TEM observation of the 316-3 specimen strained at 10% in helium at 300 K (a), 200 K (b) and 80 K (c).

manner through the region of high triaxial stresses in front of the crack tip and the rate of crack propagation is controlled by hydrogen diffusion to accumulate in the triaxial stress region. A small amount of hydrogen is generally sufficient to cause hydrogen-induced damage because it can magnify its effect by diffusion to accumulate in the potential cracking region where triaxial stress is high. Thus, HGE can only occur when external load is slowly applied for hydrogen diffusion to match crack propagation as in the present study, and is dependent on hydrogen transport process including adsorption from atmosphere and diffusion to accumulate in metals and alloys, which are determined by the microstructure and temperature.

The alloys above the Ni_{eq} of 27% showed no HGE in 1 MPa hydrogen at 200 K, where no strain-induced α' martensite was observed, in the present study. However, the alloys below the Ni_{eq} of 27% showed HGE, fracture surfaces revealed that transgranular fractures occur along α′

martensite structure, and TEM observations showed that strain-induced α' martensite is formed at the intersections of the microscopic slip bands in the grains. Thus, it is reasonable to conjecture that strain-induced α' martensite, to which the tendency of the transformation is dependent on Ni_{eq} of the alloys, plays a key role in hydrogen-induced crack propagation in the alloys.

It is well known that hydrogen transport by diffusion in the bcc lattice is several orders of magnitude rapid than in the fcc lattice. Perng and Altstetter showed that strain-induced α' martensite greatly enhanced the diffusivity of hydrogen in metastable austenitic stainless steels [34], although the equilibrium hydrogen solubility is much lower in α' martensite than in the austenitic phase [40]. Since hydrogen transport in the austenite stainless steels is almost independent of the austenite composition [41], the effects of the austenite composition can be neglected. It is considered that α' martensite provides a path for rapid hydrogen transportation in metastable austenitic stainless steels to promote hydrogen accumulation in an embrittlement region at or near the crack tip.

Since the equilibrium hydrogen solubility is much lower in α' martensite than in the austenitic phase [40], the formation of strain-induced α' martensite should result in excess hydrogen that segregates to the interfaces between the austenite phase and α' martensite. This will certainly lower the interfacial strength and may promote crack propagation along these interfaces. However, fracture surface observations of the present study indicated that transgranular fractures occurred along strain-induced martensite structure when HGE occurred in the specimen. It was supposed that the excess hydrogen in interfaces is released through the rapid diffusion path of α' martensite. The content of hydrogen that remains trapped in the interfaces of the specimen in gaseous hydrogen environment is not high enough to weaken the interfacial strength to the extend that intergranular fractures can occur along these interfaces. Thus, segregation of hydrogen to the interfaces between the austenite phase and strain-induced α' martensite does not play a key role in inducing HGE in metastable austenitic stainless steels.

The RRA of the alloys decreases with decreasing temperature, reaches a minimum at 200 K, and then increases with further decreasing temperature, as shown in Fig. 2. At temperatures above the maximum HGE temperature, the content of strain-induced α' martensite increases rapidly with decreasing temperature, as shown in Fig. 4. The hydrogen transport and consequently the susceptibility to HGE, thus, are controlled by the amount of strain-induced α' martensite in the alloy. At temperatures below the maximum HGE temperature, the strain-induced transformation of α' martensite is almost constant in the 316-1, 316-2 and 316-3 specimens, where HGE appears. This transformation behavior is in agreement with the results obtained previously by the others [42–44]. Since the hydrogen transport decreases rapidly with decreasing temperature, the accumulation of hydrogen in the region of high triaxial stress becomes more difficult in this temperature range. Thus, HGE is controlled by the slow process of hydrogen transport below the maximum HGE temperature.

Caskey found that HGE of iron–chromium–nickel alloys was dependent on nickel content, and the resistance to HGE was markedly improved in the composition range of nickel from 8% to 14% at room temperature [7]. The present study revealed that HGE decreased slowly with increasing Ni_{eq} from 24% to 26%, markedly from 26% to 27%, and then vanished above 27% with decreasing the ferrite equivalent from 47% to 0% at 200 K, as shown in Fig. 5. α' martensite formed discretely in the matrix at the early stage of deformation, as shown in Fig. 6b and c, and then grew and coalesced with increasing deformation. After coalescence, hydrogen transport can easily occur via continuous α' martensite and then HGE can occur; namely, HGE requires some amount of continuous α' martensite; thus, the resistance to HGE was markedly improved with increasing Ni_{eq}, although a small amount of α' martensite still existed. The content of strain-induced α' martensite decreases with increasing Ni_{eq} and temperature, as shown in Fig. 4, indicating that austenite can be stabilized by increasing Ni_{eq} and temperature. It is thus expected that HGE can be suppressed by increasing Ni_{eq} and temperature. The temperature dependence of the content of strain-induced α' martensite, which causes HGE, shown in Fig. 4 can contribute to improving HE resistance of austenitic stainless steels by designing Ni_{eq} for use at a given operating temperature in hydrogen energy applications.

5. Conclusions

The effect of Ni_{eq} on HGE of austenitic stainless steels of Fe–(10–20)Ni–17Cr–2Mo alloys vacuum-melted in a laboratory, based on type 316 stainless steel, was investigated by the tensile tests with a strain rate of $4.2 \times 10^{-5}\ s^{-1}$ in hydrogen and helium at 1 MPa in the temperature range from 80 to 300 K. The following conclusions were drawn on the basis of the present work:

1. HGE occurred below a Ni_{eq} of 27%, whereas no HGE occurred above the Ni_{eq} of 27%. HGE increased with decreasing temperature, reached a maximum at 200 K, and decreased with further decreasing temperature. HGE decreased slowly with increasing Ni_{eq} from 24% to 26%, markedly from 26% to 27%, and then vanished above 27% at 200 K.
2. The content of strain-induced α' martensite increased with decreasing temperature and Ni_{eq}. Hydrogen-induced fracture occurred mainly along α' martensite structure and twin boundaries. Thus, the susceptibility to HGE depended on Ni_{eq}.
3. HGE was controlled by α' martensite above the maximum HGE temperature, whereas it was controlled by the hydrogen transport below the maximum HGE temperature.

References

[1] Whiteman MB, Troiano AR. Corrosion 1965;21:53.
[2] Holzworth ML. Corrosion 1969;25:107.
[3] Hosoya Y, Inoue A, Masumoto T. J Iron Steel Inst Jpn 1978;64:89.
[4] Eliezer D, Chakrapani DG, Altstetter CJ, Pugh EN. Metall Trans A 1979;10A:935.
[5] Liu R, Narita N, Altstetter C, Birnbaum H, Pugh EN. Metall Trans A 1980;11A:1563.
[6] Holbrook JH, West AJ. In: Bernstein IM, Thompson AW, editors. Hydrogen effect in materials. Warrendale: AIME; 1981. p. 655.
[7] Caskey Jr GR. In: Louthan Jr MR, McNitt RP, Sisson Jr RD, editors. Environment degradation of engineering materials in hydrogen. Blacksburg [VA]: Virginia Polytechnic Institute; 1981. p. 283.
[8] Singh S, Altstetter C. Metall Trans A 1982;13A:1799.
[9] Abraham DP, Altstetter CJ. Metall Trans A 1995;26A:2849.
[10] Abraham DP, Altstetter CJ. Metall Trans A 1995;26A:2859.
[11] Vennett RM, Ansell GS. Trans ASM 1967;60:242.
[12] Benson Jr RB, Dann RK, Roberts Jr LW. Trans Metall Soc AIME 1968;242:2199.
[13] Walter RJ, Chandler WT. Mater Sci Eng 1969/70;5:98.
[14] Perng TP, Altstetter CJ. Metall Trans A 1987;18A:123.
[15] Han G, He J, Fukuyama S, Yokogawa K. Acta Metall 1998;46:4559.
[16] Louthan Jr MR, Caskey Jr GR, Donovan JA, Rawl Jr DE. Mater Sci Eng 1972;10:357.
[17] Thompson AW, Bernstein IM. In: Fontana MG, Staehle RW, editors. Advances in corrosion science technology, vol. 7. New York: Plenum Press; 1980. p. 3.
[18] Lagneborg R. J Iron Steel Inst 1969:363.
[19] Okada H, Hosoi Y, Abe S. Corrosion 1970;26:183.
[20] Ohtani N, Asano S, Fujishima Y, Yamamasu Y. J Jpn Inst Met 1973;37:746.
[21] Briant CL. Metall Trans A 1979;10A:181.
[22] Hänninen H, Hakkarainen T. Metall Trans A 1979;10A:1196.
[23] Hänninen H, Hakkarainen T. Corrosion 1980;36:47.
[24] Eliezer D. J Mater Sci 1984;19:1540.
[25] Rozenak P. J Mater Sci 1990;25:2532.
[26] Buckley JR, Hardie D. Mater Sci Technol 1993;9:259.
[27] Louthan Jr MR. In: Bernstein IM, Thompson AW, editors. Hydrogen in metals. AIME; 1976. p. 53.
[28] Perra MW. In: Louthan Jr MR, McNitt RP, Sisson Jr RD, editors. Environment degradation of engineering materials in hydrogen. Blacksburg [VA]: Virginia Polytechnic Institute; 1981. p. 321.
[29] Stoltz RE, Moody NR, Perra MW. Metall Trans A 1983;14A:1528.
[30] Schuster G, Altstetter C. Metall Trans A 1983;14A:2085.
[31] Sun D, Han G, Vaodee S, Fukuyama S, Yokogawa K. Mater Sci Technol 2001;10:302.
[32] Fukuyama S, Sun D, Zhang L, Wen M, Yokogawa K. J Jpn Inst Met 2003;67:456.
[33] Narita N, Birnbaum HK. Scripta Metall 1980;14:1355.
[34] Perng TP, Altstetter CJ. Acta Metall 1986;34:1771.
[35] Wayman ML, Smith GC. Metall Trans 1970;1:1189.
[36] Hirayama T, Ogirima M. J Jpn Inst Met 1970;34:507.
[37] Han G, He J, Fukuyama S, Yokogawa K. Rev Sci Instrum 1997;68:4232.
[38] Nelson HG. In: Raymond L, editor. Hydrogen embrittlement testing. STP 543. Philadelphia [PA]: ASTM; 1974 p. 152.
[39] Troiano AR. ASM Trans 1960;52:54.
[40] Nelson HG. Treatise Mater Sci Technol 1983;25:275.
[41] Louthan Jr MR, Derrick RG. Corrosion Sci 1975;15:565.
[42] Angel T. J Iron Steel Inst 1954;177:165.
[43] Olson GB, Cohen M. Metall Trans A 1975;6A:791.
[44] Hecker SS, Stout MG, Staudhammer KP, Smith JL. Metall Trans A 1982;13A:619.